

# **Orbiting Carbon Observatory-2 & 3 (OCO-2 & OCO-3)**



## **Orbiting Carbon Observatory-3 (OCO-3) Data Quality Statement: Level 2 Forward and Retrospective Processing Data Release 10 (v10 and v10r), v10.4 Lite Files**

Version 3.0 Rev 1  
April 18, 2022

National Aeronautics and  
Space Administration



Jet Propulsion Laboratory  
California Institute of Technology  
Pasadena, California

# **Orbiting Carbon Observatory-3 (OCO-3) Data Quality Statement: Level 2 Forward Processing Data Release 10 (v10)**

Abhishek Chatterjee

Vivienne Payne

Annmarie Eldering

Robert Rosenberg

Matthäus Kiel

Brendan Fisher

Robert Nelson

Lan Dang

Graziela Keller Rodrigues

Christopher O'Dell

Tommy Taylor

Gregory Osterman

Jet Propulsion Laboratory

Jet Propulsion Laboratory

Jet Propulsion Laboratory

Jet Propulsion Laboratory

Jet Propulsion Laboratory

Jet Propulsion Laboratory

Jet Propulsion Laboratory

Jet Propulsion Laboratory

Jet Propulsion Laboratory

Colorado State University

Colorado State University

Jet Propulsion Laboratory

**Document History:**

<b>Version</b>	<b>Revision</b>	<b>Date</b>	<b>Description/Comments</b>
1.0	1	April 30, 2020	Data Quality Statement for OCO-3 vEarly
2.0	1	August 1, 2021	Updated for new data release, v10
2.0	2	September 2, 2021	Minor revisions and notes on v10r
3.0	1	April 18, 2022	Update for v10.4r data release

The research described in this document was carried out at the Jet Propulsion Laboratory, California Institute of Technology, under a contract with the National Aeronautics and Space Administration.  
Copyright 2022. All rights reserved.

**TABLE OF CONTENTS**

1	Data Quality Statement for the OCO-3 Level 2 Data Product .....	1
2	Key differences between v10 and vEarly .....	3
2.1	Radiometric errors .....	3
2.2	Geolocation errors.....	4
3	Validation Status .....	6
4	Summary.....	7
5	Selected References.....	8
6	Links .....	10

### LIST OF FIGURES

Figure 1-1: Showing the updated bias correction and the improvement in dXCO<sub>2</sub>. Compare the value of dXCO<sub>2</sub> at the top of the figure (prior to the new bias correction) to that at the bottom (corrected). The middle of the figure shows the OCO-3 ZLO and the adjustment in XCO<sub>2</sub> with time (orbit number). ..... 2

Figure 2-1: Lamp radiance trends relative to prelaunch over the course of the OCO-3 mission. The three panels are for the ABO<sub>2</sub>, WCO<sub>2</sub>, and SCO<sub>2</sub> channels. Within each panel, different colors indicate different lamps. Lamp 3 is used roughly 12 times per day, Lamp 2 is used roughly 3 times per day, and Lamp 1 is used roughly 1 time per week. .... 3

Figure 2-2: L2 dP values from OCO-3 v10 test data from Aug 2019 to Dec 2020. .... 4

## **LIST OF TABLES**

**No tables found.**

## 1 Data Quality Statement for the OCO-3 Level 2 Data Product

The Orbiting Carbon Observatory (OCO-3) has released an updated version of the Level 2 (L2) Lite file data product, containing estimates of the column averaged carbon dioxide dry air mole fraction ( $X_{CO_2}$ ) and other geophysical quantities retrieved from OCO-3 observations. This updated version of the L2 Lite file data product is release 10.4r (v10.4r). A full reprocessing of the OCO-3 L2 Lite data set has been completed with data going back to the beginning of mission data record in August 2019 and the data available at the Goddard Earth Sciences Data and Information Services Center later in 2022. Updated documentation, particularly the L2 Data User's Guide, will be made available in the near future.

The v10.4r Lite file release addresses a problem with the v10r  $X_{CO_2}$  data. The new Lite file data version was necessary because it was noticed during routine validation of the v10r data product that a time dependent bias could be seen in the OCO-3  $X_{CO_2}$  data compared to collocated OCO-2 observations ( $dX_{CO_2}$ ). The magnitude of the bias is correlated with the amount of time between instrument decontamination cycles, and so is assumed to be associated with icing on the OCO-3 detectors. One proxy for the build-up of ice on the detectors is an instrument calibration metric called the zero-level-offset (ZLO). For OCO-3, ZLO is measured for both the weak  $CO_2$  and the  $O_2$  A-band, but the weak  $CO_2$  band measurements of ZLO are less noisy, making them a more convenient metric than A-band ZLO. A bias correction term was calculated from a fit of  $dX_{CO_2}$  to the ZLO from the weak  $CO_2$  band. Comparisons between the new bias corrected  $X_{CO_2}$  data and data from the Total Carbon Column Observation Network show that v10.4r Lite  $X_{CO_2}$  data is minimally affected by the time dependence related to build up of ice on the detectors. Comparisons of OCO-3 data to OCO-2  $X_{CO_2}$  also show that the effects of the ice build up have been resolved by the updated bias correction. The impact and magnitude of the correction can be seen in Figure 1-1. We have also completed validation of the OCO-3 v10.4r Lite products against TCCON and multimodel median, showing over all good agreement with these truth proxies – more details on these are available in Section 3

The OCO-3 v10.4r Lite data product should be used instead of the previous v10r Lite. Note that the time-dependent  $X_{CO_2}$  correction for the v10.4r product comes in via the Level 2 bias correction. (Improvements between the previous OCO-3 v10r and vEarly data products were achieved via updates to the Level 1b radiometric calibration and geolocation.)

Users should be aware that the geolocation of the retrospective product in some cases will be superior to the forward stream of the data.

The L2 algorithms used to create the OCO-3 data are the same as those that are used for the current OCO-2 v10 L2 data release, to aid in the use of the two datasets together.

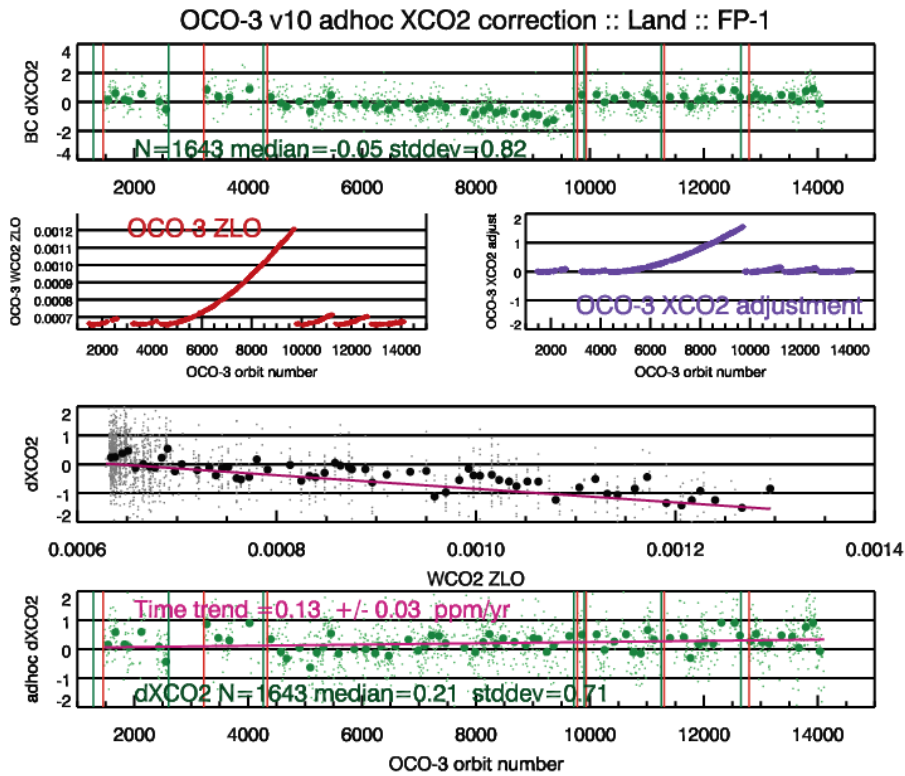


**Figure 1-1:** Showing the updated bias correction and the improvement in dXCO2. Compare the value of dXCO2 at the top of the figure (prior to the new bias correction) to that at the bottom (corrected). The middle of the figure shows the OCO-3 ZLO and the adjustment in XCO2 with time (orbit number).



## 2 Key differences between v10 and vEarly

### 2.1 Radiometric errors

The radiometric calibration of v10 was significantly improved compared to vEarly. In contrast to vEarly, which contains a discontinuity at April 8, 2020, all lamp data across the entire mission is now processed with the same algorithms. The key improvement for v10 was to tie radiometric degradation to Lamp 1, which is used roughly once a week. Initially, Lamp 3 was being used with no correction for lamp aging. Additionally, v10 featured an updated stray light model which aims to account for spatial variability.

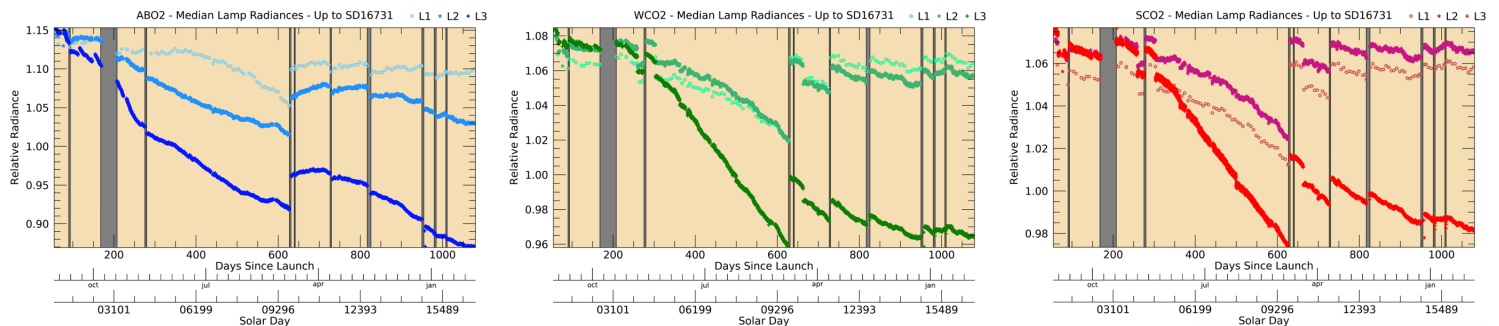


**Figure 2-1:** Lamp radiance trends relative to prelaunch over the course of the OCO-3 mission. The three panels are for the ABO2, WCO2, and SCO2 channels. Within each panel, different colors indicate different lamps. Lamp 3 is used roughly 12 times per day, Lamp 2 is used roughly 3 times per day, and Lamp 1 is used roughly 1 time per week.

Since the focal plane arrays are operated at cryogenic temperatures, ice accumulates over time, leading to increased stray light and decreased throughput. Several decontaminations have been performed to counteract this. The largest discontinuity in the gain degradation record (Figure 2-1) occurs following the decon from solar day 9720, which was nearly a year after the previous one.

A key indicator of calibration improvements was a reduction in time dependent and footprint dependent behavior in the L2 data in v10 compared to vEarly. The science team examined the behavior of  $dP$ , the difference between the retrieved and prior surface pressure, a parameter in the retrieval that is very sensitive to ABO2 radiometric calibration. We found that this parameter was more stable in v10 than in vEarly, although an increase in value correlated with detector icing remained. A clear increase is visible between June 2020 and Jan 2021. The  $dP$  test data record shown in **Error! Reference source not found.** ends in Dec 2020, just before a major decontamination event.

In addition to the time dependence, there is some variation in the  $dP$  values among footprints, which is consistent with our understanding that icing impacts are spatially nonuniform, but the magnitude in v10 is substantially reduced from vEarly. This is also seen in the throughput of data in L2 which worsened later in the vEarly record, especially for high numbered footprints. This pattern is not seen in v10.

Since the release of the OCO-3 v10 dataset, the team has continued to further characterize Level 1B calibration. The v10.4r Lite products incorporate an ad hoc correction to the Level 2  $X_{CO_2}$  that aims to account for outstanding issues in the Level 1B calibration.

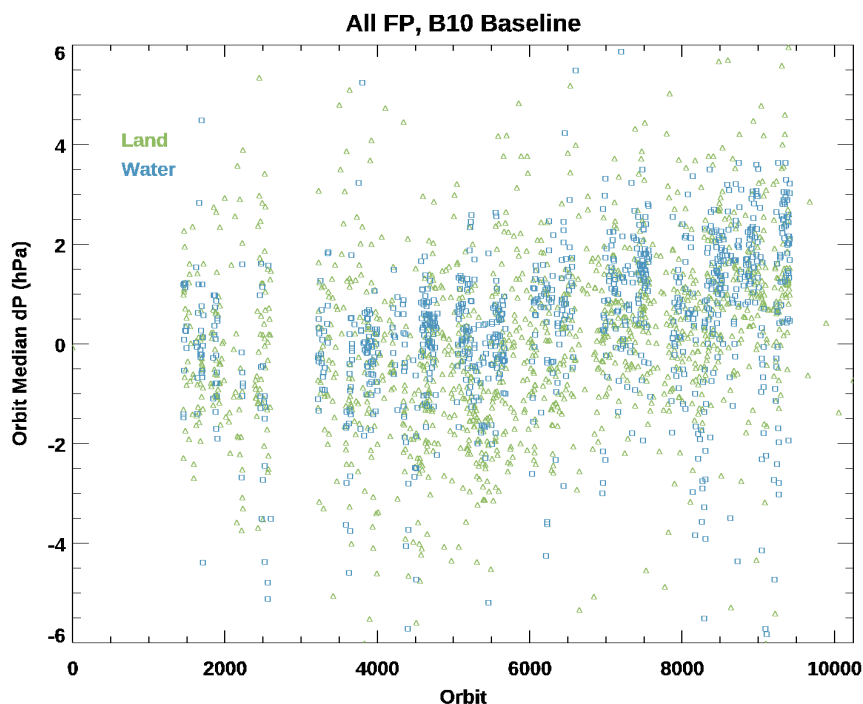


Figure 2-2: L2 dP values from OCO-3 v10 test data from Aug 2019 to Dec 2020.

## 2.2 Geolocation errors

Geolocation errors were substantially improved for v10 compared to vEarly in three general areas. First, calibration of the Pointing Mirror Assembly (PMA) was completed and integrated directly into the geolocation algorithm. Second, an offset between the science detectors and the PMA camera was characterized and removed. Third, the OCO-3 project obtained a supplemental attitude source, derived from the CALET instrument which is near OCO-3 on the JEM-EF, for periods when the OCO-3 Stellar Reference Unit (SRU) is not available. The supplemental attitude data reduces geolocation errors associated with flexure between the ISS center, where the primary ISS ephemeris is reported, and the OCO-3 location on the JEM-EF. For periods when the OCO-3 SRU is available, geolocation errors are typically less than 500 m. For periods where the SRU is not available and CALET-derived attitude is available, errors are typically less than 1 km. Finally, a small percentage of the data remains when neither of the two primary attitude sources are available, and for these periods the errors are typically less than 2 km, with a small “tail” with errors up to 3 km. Starting with v10, the OCO-3 L2 products contain a field called `/RetrievalGeometry/retrieval_att_data_source`. A value of 1 in this field represents the “no supplemental attitude” case, with the largest errors. Other values in the range 2-9, have good geolocation, with the errors listed above. The different numbers in the 2-9 range represent various permutations of SRU and CALET, accounting for nominal operations with the possibility of small gaps.

The improvements that rely on the CALET data are only available in the retrospective processing (v10r). In the forward stream processing, we rely solely on the OCO-3 SRU and ISS BAD data, so geolocation performance may be poorer than in the retrospective data. The attitude source information that is included in the product can help the user to differentiate these cases. More details will be in the Data User's Guide.

### 3 Validation Status

The fundamental means for tying the OCO-3  $X_{CO_2}$  to the World Meteorological Organization's  $CO_2$  standard is by comparison with ground-based observations from the Total Carbon Column Observing Network (TCCON). A description of the process of validating OCO-2 data against TCCON is described in Wunch et al. (2017) using an earlier OCO-2 data version. The OCO-2 validation plan was first described prior to launch in an analysis using TCCON and  $X_{CO_2}$  estimates retrieved using the OCO-2 retrieval algorithm on data from JAXA's GOSAT satellite (Wunch et al, 2011b). To derive quality filtering and bias correction, we follow the methods described in O'Dell et al. (2018). We compare the retrieved  $X_{CO_2}$  to an independent estimate of  $X_{CO_2}$ , a so-called truth proxy. For OCO-3 v10, we used three different truth proxy data sets: TCCON, a small area approximation (SAA), and a truth proxy based on results from global carbon flux inverse models ("multi-model median").

The TCCON truth proxy includes data from 19 TCCON stations. We use the GGG2014 dataset covering the time period between August 2019 and December 2020 and spanning from 55°N to 45°S in latitude. We use similar coincidence criteria as O'Dell et al., (2018) to match airmasses observed by TCCON and OCO-3. In total we count ~101K coincident soundings between OCO-3 and TCCON in nadir mode over land, ~91K coincident soundings in SAM/target mode, and 18K soundings in glint mode over water.

The SAA truth proxy (for more details see O'Dell et al.,2018) makes use of the low spatial variability of  $X_{CO_2}$  over small regions (up to 100 km) and short time spans (~10 s). Here we define continuous segments of soundings that were collected along-track within ~10 s as small areas. Between August 2019 and December 2020, the SAA truth proxy consists of ~656K soundings in nadir mode over land, ~219K soundings in SAM/target mode, and ~ 869K soundings in glint mode over water.

A suite of four models sampled at OCO-3 sounding locations and times was used for the multi-model median truth proxy (for more details see O'Dell et al.,2018). The models generally differ in their prior flux assumptions, prior flux uncertainty, transport model, initial conditions, spatial resolution, and inverse method. Each model assimilates either in-situ  $CO_2$  concentration data, GOSAT  $X_{CO_2}$  data, OCO-2  $X_{CO_2}$  data, or a combination of the above. Between August 2019 and December 2020, the multi-model median truth proxy consists of ~1358K soundings in nadir mode over land, ~797K soundings in SAM/target mode, and ~ 1500K soundings in glint mode over water.

All three truth proxy data sets were used to derive quality filters, which utilize different parameters within the L2 data product. Further, a footprint and parametric bias correction formula has been determined that allows for adjusting the OCO-3 data consistent with biases seen relative to the truth proxy data sets. In addition, for observations over land, a global scaling factor of 0.9963 was determined to tie OCO-3  $X_{CO_2}$  data to the WMO  $CO_2$  standard scale (through direct comparisons to TCCON). For observations over water, a global scaling factor of 0.9961 was determined (using a multi-model median and coastline bootstrap method).

A first comparison between co-located TCCON and filtered and bias corrected  $X_{CO_2}$ , indicates a single sounding root mean squared error (RMSE) of 1.33 ppm for nadir observations over land, 1.31 ppm for SAM/target observations, and 0.99 ppm for glint observations over water. The v10 bias correction also reduces swath biases that were apparent in OCO-3's vEarly SAM and target mode observations.

## 4 Summary

Overall, OCO-3 v10  $X_{CO_2}$  shows very good performance for all three modes of data collection. A more detailed validation and evaluation study of OCO-3  $X_{CO_2}$  against TCCON, model data, COCCON, and cross comparisons against OCO-2 will be included in the Data User's Guide. The OCO-2 and OCO-3 data are now both released in v10, which will support the science community in the use of the datasets together.

There is more documentation that will help with utilizing the OCO-3 L2 data, all of which is available at the GES DISC OCO-3/OCO-2 documentation page (<https://disc.gsfc.nasa.gov/information/documents?title=OCO-2%20Documents>). Note that OCO-2 and OCO-3 have combined documents. For example, the L2 ATBD will describe the common algorithm as well as mission specific features and the small number of differences in the data fields. The Level 2 Data User's Guide is also a combined document with information about data fields, data filtering and bias correction.

## 5 Selected References

- Chatterjee, A., et al. (2017), Influence of El Niño on atmospheric CO<sub>2</sub> over the tropical Pacific Ocean: Findings from NASA's OCO-2 mission, *Science* 358, DOI: [10.1126/science.aam5776](https://doi.org/10.1126/science.aam5776).
- Crisp, D., et al. (2004), The Orbiting Carbon Observatory (OCO) mission, *Advances in Space Research* 34 700–709, DOI: [10.1016/j.asr.2003.08.062](https://doi.org/10.1016/j.asr.2003.08.062).
- Crisp, D., et al. (2012), The ACOS  $X_{CO_2}$  retrieval algorithm, Part 2: Global  $X_{CO_2}$  data characterization, *Atmos Meas. Tech.*, 5, 687-707, DOI: [10.5194/amt-5-687-2012](https://doi.org/10.5194/amt-5-687-2012).
- Crisp, D., et al. (2017), Improved retrievals of carbon dioxide from Orbiting Carbon Observatory-2 with the version 8 ACOS algorithm, *Atmos Meas. Tech.*, 10, 1, 59-81, DOI: [10.5194/amt-10-59-2017](https://doi.org/10.5194/amt-10-59-2017).
- Eldering, A., et al. (2017), The Orbiting Carbon Observatory-2 early science investigations of regional carbon dioxide fluxes, *Science*, 358, 6360, DOI: [10.1126/science.aam5745](https://doi.org/10.1126/science.aam5745).
- Eldering, A. et al. (2019), The OCO-3 mission: measurement objectives and expected performance based on 1 year of simulated data, *Atmos. Meas. Tech.*, 12, 4, 2341-2370, DOI: [10.5194/amt-12-2341-2019](https://doi.org/10.5194/amt-12-2341-2019).
- Frankenberg, C., et al. (2011), New global observations of the terrestrial carbon cycle from GOSAT: Patterns of plant fluorescence with gross primary productivity, *Geophysical Research Letters*, 38, L17706 DOI: [10.1029/2011GL048738](https://doi.org/10.1029/2011GL048738).
- Frankenberg, C., et al. (2012), Remote sensing of near-infrared chlorophyll fluorescence from space in scattering atmospheres: implications for its retrieval and interferences with atmospheric CO<sub>2</sub> retrievals, *Atmospheric Measurement Techniques*, 5(8), 2081–2094, DOI: [10.5194/amt-5-2081-2012](https://doi.org/10.5194/amt-5-2081-2012).
- Hakkarainen, J., et al. (2016), Direct space-based observations of anthropogenic CO<sub>2</sub> emission areas from OCO-2, *Geophysical Research Letters*, 43(21), 11400-11406, DOI: [10.1002/2016GL070885](https://doi.org/10.1002/2016GL070885).
- Kiel M. et al. (2019), How bias correction goes wrong: measurement of X-CO<sub>2</sub> affected by erroneous surface pressure estimates, *Atmospheric Measurement Techniques* 12, 4, 2241-2259, DOI: [10.5194/amt-12-2241-2019](https://doi.org/10.5194/amt-12-2241-2019).
- Liu, J., et al. (2017), Contrasting carbon cycle responses of the tropical continents to the 2015–2016 El Niño. *Science* 358, 6360, DOI: [doi:10.1126/science.aam5690](https://doi.org/10.1126/science.aam5690).
- Nelson, R., et al. (2016), High-accuracy measurements of total column water vapor from the Orbiting Carbon Observatory-2, *Geophysical Research Letters*, 43, 12261-12269, DOI: [10.1002/2016GL071200](https://doi.org/10.1002/2016GL071200).
- Nelson, R., et al. (2020), Retrieved wind speed from the Orbiting Carbon Observatory-2. *Atmospheric Measurement Techniques* 13, 12, 6889-6899, DOI: [10.5194/amt-13-6889-2020](https://doi.org/10.5194/amt-13-6889-2020).
- O'Dell, C. et al. (2018), Improved retrievals of carbon dioxide from Orbiting Carbon Observatory-2 with the version 8 ACOS algorithm, *Atmospheric Measurement Techniques*, 11,12, 6539–6576, DOI: [10.5194/amt-11-6539-2018](https://doi.org/10.5194/amt-11-6539-2018).

- O'Dell, C. et al. (2012), The ACOS CO<sub>2</sub> retrieval algorithm – Part 1: Description and validation against synthetic observations, *Atmospheric Measurement Techniques*, 5,1, 99-121, DOI: [10.5194/amt-5-99-2012](https://doi.org/10.5194/amt-5-99-2012).
- Sun, Y., et al. (2017), OCO-2 advances photosynthesis observation from space via solar-induced chlorophyll fluorescence *Science*, 358, 6360, DOI: [10.1126/science.aam5747](https://doi.org/10.1126/science.aam5747).
- Wunch D. et al. (2010), Calibration of the Total Carbon Column Observing Network using aircraft profile data, *Atmospheric Measurement Techniques*, 3, 5, 1351–1362, DOI: [10.5194/amt-3-1351-2010](https://doi.org/10.5194/amt-3-1351-2010).
- Wunch D. et al. (2011a), The Total Carbon Column Observing Network, *Phil. Trans. R. Soc. A*, 369, 2087–2112, DOI: [10.1098/rsta.2010.0240](https://doi.org/10.1098/rsta.2010.0240).
- Wunch D. et al. (2011b), A method for evaluating bias in global measurements of CO<sub>2</sub> total columns from Space, *Atmos. Chem. Phys. Discuss.*, 11, 20899-20946, DOI: [10.5194/acpd-11-20899-2011](https://doi.org/10.5194/acpd-11-20899-2011).
- Wunch D. et al. (2017), Comparisons of the Orbiting Carbon Observatory-2 (OCO-2)  $X_{CO_2}$  Measurements with TCCON, *Atmos. Meas. Tech. Discuss.*, 10, 2209-2238, DOI: [10.5194/amt-10-2209-2017](https://doi.org/10.5194/amt-10-2209-2017).

## 6 Links

- OCO-2 Mission [web site](#)
- OCO-2 L2 v10 Standard Data summary page at the Goddard DISC: [link](#)
- Related: OCO-3 Mission [web site](#)
- Related: OCO-3 L2 v10.4 Lite File page at the Goddard DISC [page](#)
- Related: JPL retrievals using the radiances from the Japanese GOSAT satellite, known as the Atmospheric CO2 Observations from Space (ACOS) data at the Goddard DISC [page](#)